IIE Transactions (2006) **38**, 341–354

ISSN: 0740-817X print / 1545-8830 online
DOI: 10.1080/07408170500216498

Signature construction and matching for fault diagnosis in manufacturing processes through fault space analysis

NONG JIN and SHIYU ZHOU

Department of Industrial and Systems Engineering, University of Wisconsin, Madison, WI 53706, USA
E-mail: szhou@engr.wisc.edu

Received August 2004 and accepted May 2005

Variation-source identification in manufacturing processes is highly desired since it enables improvements in product quality. Recently, data-driven variation-source identification has received considerable attention. This paper presents a systematic variation-source identification method by assuming a linear model between the quality measurements and process faults. The noise term in the model is assumed to have a simple form. The variation-source identification is achieved through the testing of the common eigenspace between the fault signatures and the covariance matrix of the newly collected samples. Three types of fault signatures are constructed from either one or two covariance matrices for pattern matching. A systematic procedure to construct the signature is presented. A case study of a machining operation is conducted to illustrate the effectiveness of the proposed methodology.

1. Introduction

Statistical process control (SPC) (Montgomery and Woodall, 1997) is a popular technique used in practice for quality improvement. However, SPC possesses limited diagnosis capabilities to identify the variation sources after quality changes are detected. Woodall and Montgomery (1999) highlighted variation-source identification as an important research direction in SPC. Consider the following example of a machining operation (Fig. 1(a–c)). The workpiece is a cube of metal (only the front view is shown). Surface C of the workpiece is milled in the first step (Fig. 1(a)). In the second step, a hole is drilled into surface D (Fig. 1(b)) with the workpiece being located in the fixture. Clearly, the resulting hole is not perpendicular to surface D (Fig. 1(c)) due to a fixture error. The fixture error could be a mean shift in the locating pin height due to an error during set up or a variance increase in the locating pin height due to the pin becoming loose. In most cases, the mean-shift error can be easily compensated even without knowing the error sources. For example, if the drilled hole always deviates from 90° by a fixed value, the angle between the drill and the fixture can be adjusted to compensate for this deviation without removing the fixture error. The error of variation increase is much more difficult to remove. The sources of this variation increase, so-called "variation sources", often need to be identified before being eliminated. One point needing to be clarified here is that there are many sources in a process that cause variation. However, only those sources that cause excessive variation are defined as "variation sources" in this paper. Therefore, variation sources are also called "process faults." The quality change can be detected using the SPC technique, however, fault diagnosis is often left to the operator and the troubleshooting activities are mainly based on experience.

In practice, it is highly desirable to develop systematic methodologies to identify the variation sources from process/product information. Significant developments in computer and sensing technologies provide us with great opportunities in this research direction. Extensive measurement data on manufacturing processes are now often readily available. In some manufacturing processes such as autobody assembly processes, 100% dimension inspection has been achieved through in-line optical coordinate measurement machines (Ceglarek and Shi, 1995). However the existence of extensive data sets means that the questions of how to efficiently retrieve useful information and then relate them to the variation sources have become increasingly important.

Several linear models have been proposed to link the quality measurement data and the variation sources (Jin and Shi, 1999; Mantripragada and Whitney, 1999; Ding *et al.*, 2000;, Huang *et al.*, 2000; Camelio *et al.*, 2003; Djurdjanovic and Ni, 2001; Zhou *et al.*, 2003). These linear models can be put in the following generic form:

$$\mathbf{y} = \mathbf{A}\mathbf{f} + \varepsilon, \tag{1}$$

where $\mathbf{y}$ is a vector consisting of product quality measurements that are the deviations of quality characteristics from their nominal values, $\mathbf{A}$ is a constant coefficient matrix determined by the process/product design, $\mathbf{f}$ is a vector that represents the process variation sources, and ε includes the

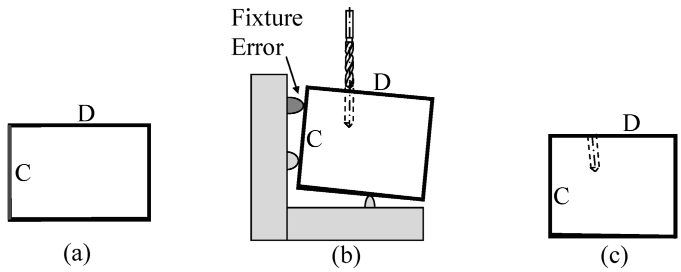

Fig. 1. Effect of fixture error on product dimensional quality: (a) the first step of milling the workpiece; (b) a hole is drilled; (c) clearly the hole is not perpendicular to surface D.

measurement noise and unmodeled variations. The above mentioned fault-quality model is derived from the first principles of the process. These models can provide useful insights into the link between the variation sources and product-quality measurements. However, the physics of the process need to be thoroughly studied if a valid process model is to be produced, which is usually very difficult, if not impossible, for a large-scale system (Chiang *et al.*, 2001).

Data-driven models do not require much *a priori* knowledge on the manufacturing process. Instead, data-driven models focus on investigating patterns in the extensive historical data sets to estimate the coefficient matrix **A**. Apley and Shi (2001) presented a descriptive method that is able to extract and interpret information from the quality data by assuming that the coefficient matrix **A** in Equation (1) has a ragged lower-triangular form. The physical interpretations of the faults are pursued after **A** is estimated. Later, Apley and Lee (2003) proposed a blind separation approach to identify spatial variation patterns in manufacturing data. Some specific autocorrelation or distribution conditions are required on the variation sources and process noise to apply these techniques. Most recently, Jin and Zhou (2005) proposed a method to estimate the column vectors of the **A** matrix using a gradual learning procedure. This procedure is based on the fact that if only one variation source exists (only one nonzero component in **f**), and the covariance of $\boldsymbol{\varepsilon}$ is in the form of $\sigma^2\mathbf{I}$, **I** being the identity matrix, then the eigenvector associated with the largest eigenvalue of $\boldsymbol{\Sigma}_\mathbf{y}$, the covariance matrix of **y**, is then the same as the column of **A** that corresponds to the nonzero component of **f**. Thus, the column vectors of **A** can be obtained when a single fault occurs in the system and can be stored as signatures of the corresponding variation sources in a library.

Signature matching is a popular method to identify variation sources based on quality measurement data after the fault-quality model has been built. In many available signature matching techniques including those of Ceglarek and Shi (1996), Rong *et al.* (2000), and Ding *et al.* (2002) the columns of **A** are treated as the signatures of corresponding faults and it is assumed that during the data collection period, only one fault occurs in the system. In their approach, the eigenvector associated with the largest eigenvalue of $\mathbf{S}_\mathbf{y}$, the sample covariance matrix of **y**, is calculated and compared with the columns of **A** that are either derived through a physical analysis of the process or estimated based on the historical data. If there is a match, then the corresponding fault happened in the system. Fisher Discrimination Analysis (FDA) (Russell and Braatz, 1998) classifies the scattered groups in the historical data and treats a group as a signature of an individual fault. The advantage of this method is that it may provide fast fault diagnosis since it does not need to wait for the accumulation of new samples to construct a covariance matrix before diagnosis. The FDA method is used mainly in mean-shift detection and may have difficulty dealing with unknown faults since there is no predefined discriminate function for those unknown faults. In addition, since each discriminant function is defined for one particular fault only, how to apply this approach to the case where multiple faults happen simultaneously is not clear. In Jin and Zhou (2005), signature matching is extended to the multiple-fault case. In their method, the identification of multiple variation sources was achieved by comparing the space spanned by the eigenvectors associated with large eigenvalues of $\mathbf{S}_\mathbf{y}$ and the space spanned by the fault signatures in a fault library. Although signature matching can be conducted under a multiple-fault condition, the signature construction procedure still needs the single-fault condition in that method.

In this paper, we develop a systematic technique to construct the signatures of process faults and a rigorous testing procedure to identify the variation sources through signature matching. There are two salient features of the proposed technique: (i) we discard the traditional method of using column vectors of **A** as fault signatures. Instead, we treat each sample covariance matrix under a fault condition as a fault signature. The method can construct fault signatures not only when a single fault exists in the system, but also when multiple faults occur simultaneously; and (ii) the testing statistics for signature matching have analytical expression and thus the testing performance will not be influenced by the values of **A**.

This paper is structured as follows. In Section 2, the problem formulation, the method of signature construction, and the procedures of variation-source identification and performance evaluations (study on the type-I error) on the proposed procedures are presented. A complete procedure is developed that is able to quickly identify the process-variation sources. A case study is illustrated in Section 3 to demonstrate the effectiveness of this technique. Conclusions are presented in Section 4.

2. Signature construction and variation-source identification

2.1. *Problem formulation*

In this paper, we adopt a linear relationship between the process faults and product quality, as shown in

Equation (1). Although the relationship between $\mathbf{y}$ and $\mathbf{f}$ is in general nonlinear, a linear relationship can provide a good approximation because the process faults are often small in magnitude. In this paper, the following assumptions are made in solving Equation (1):

1. $\mathbf{A}$ is an *unknown* m by k matrix. The columns of $\mathbf{A}$ are linearly independent.
2. $\mathbf{f}$ is a k by 1 vector that follows a multivariate normal distribution $N(\mathbf{0}, \mathbf{D})$, where $\mathbf{D}$ is a diagonal matrix. The components of $\mathbf{f}$ are assumed to be independent because the process faults are often independent of one another.
3. $\boldsymbol{\varepsilon}$ is an m by 1 vector that follows a multivariate normal distribution $N(\mathbf{0}, \sigma^2\,\mathbf{I})$, where σ^2 is a scalar and $\mathbf{I}$ is the identity matrix. Furthermore, we assume that $\boldsymbol{\varepsilon}$ is independent of $\mathbf{f}$. This assumption is reasonable if the same measurement device is used to measure all the quality characteristics. For example, if we use the same Coordinate Measurement Machine (CMM) to measure the positions of many points on a car body, the covariance of the measurement errors of these points can be viewed in this form. The same assumption has been discussed and adopted by many researchers, such as Ceglarek and Shi (1996), Rong *et al.* (2000), and also Apley and Shi (2001).

Based on this linear model, the problem of variation-source identification can be formulated as follows. Given multiple observations of $\mathbf{y}$, how do we identify which faults happen?

To analyze Equation (1), we take the covariance of both sides and get:

$$\boldsymbol{\Sigma}_{\mathbf{y}} = \mathbf{A}\boldsymbol{\Sigma}_{\mathbf{f}}\mathbf{A}^T + \sigma^2\mathbf{I}. \tag{2}$$

where $\boldsymbol{\Sigma}_{\mathbf{y}}$ is the population covariance matrix of $\mathbf{y}$ (the m-dimensional quality measurements) and $\boldsymbol{\Sigma}_{\mathbf{f}}$ is the covariance matrix of $\mathbf{f}$. It is known that if k faults exist in the system, we will have $\lambda_1 \geq \lambda_2 \geq \ldots \geq \lambda_k \geq \sigma^2 = \lambda_{k+1} = \ldots = \lambda_m$, where λ_i, $i = 1 \ldots m$, are the eigenvalues of $\boldsymbol{\Sigma}_{\mathbf{y}}$. A straightforward analysis can show that the k eigenvectors associated with the first k largest eigenvalues of $\boldsymbol{\Sigma}_{\mathbf{y}}$ span the same linear space of the k column vectors of the $\mathbf{A}$ matrix corresponding to the k faults (Apley and Shi, 2001). This result possesses a very important implication: if the same k faults happen in the system, then the first k eigenvectors of $\boldsymbol{\Sigma}_{\mathbf{y}}$ should span the same linear space. Based on this implication, a new technique for the construction and identification of fault signatures can be developed. First, we introduce some terminologies.

- *Fault vectors* and *fault space*. If k ($k > 0$) faults occur simultaneously in the system, then the k eigenvectors associated with the k largest eigenvalues ($\lambda_1, \lambda_2, \ldots, \lambda_k$) of $\boldsymbol{\Sigma}_{\mathbf{y}}$ are called the fault vectors of $\boldsymbol{\Sigma}_{\mathbf{y}}$ and the space spanned by the k eigenvectors is called the fault space of $\boldsymbol{\Sigma}_{\mathbf{y}}$, which will be denoted as $\mathcal{F}(\boldsymbol{\Sigma}_{\mathbf{y}})$. For the sake of convenience, in this paper, "the fault space of $\boldsymbol{\Sigma}_{\mathbf{y}}$" is equivalent to "the fault space spanned by all the fault vectors of $\boldsymbol{\Sigma}_{\mathbf{y}}$". Because eigenvectors of a real symmetric matrix are real and orthogonal to one another, the dimension of $\mathcal{F}(\boldsymbol{\Sigma}_{\mathbf{y}})$ is M-dimensional if and only if the number of fault vectors of $\boldsymbol{\Sigma}_{\mathbf{y}}$ is equal to M. The dimension of $\mathcal{F}(\boldsymbol{\Sigma}_{\mathbf{y}})$ is denoted as $\dim(\mathcal{F}(\boldsymbol{\Sigma}_{\mathbf{y}}))$.
- *Equivalence of two fault spaces*. Two fault spaces $\mathcal{F}(\boldsymbol{\Sigma}_1)$ and $\mathcal{F}(\boldsymbol{\Sigma}_2)$ (without causing confusion, $\boldsymbol{\Sigma}_{\mathbf{y}_i}$ is simplified as $\boldsymbol{\Sigma}_i$) are said to be equivalent if and only if the fault vectors of $\boldsymbol{\Sigma}_1$ and $\boldsymbol{\Sigma}_2$ span the same space, denoted as $\mathcal{F}(\boldsymbol{\Sigma}_1) = \mathcal{F}(\boldsymbol{\Sigma}_2)$. It is important to note that if two fault spaces are equivalent, then the dimension of the two fault spaces should also be equal.
- *Operations of fault spaces*. Given two fault spaces $\mathcal{F}(\boldsymbol{\Sigma}_1)$ and $\mathcal{F}(\boldsymbol{\Sigma}_2)$, the sum space of the two fault spaces is the overall space spanned by all the independent fault vectors from both fault covariance matrices $\boldsymbol{\Sigma}_1$ and $\boldsymbol{\Sigma}_2$, and it is denoted as $\mathcal{F}(\boldsymbol{\Sigma}_1)+\mathcal{F}(\boldsymbol{\Sigma}_2)$. The dimension of the sum space of two fault spaces is the total number of all the independent fault vectors from both fault covariance matrices. Obviously, $\dim(\mathcal{F}(\boldsymbol{\Sigma}_1)+\mathcal{F}(\boldsymbol{\Sigma}_2)) \leq \dim(\mathcal{F}(\boldsymbol{\Sigma}_1)) + \dim(\mathcal{F}(\boldsymbol{\Sigma}_2))$, and if two fault spaces are equivalent, then the dimension of the sum space of the two fault spaces should be equal to the dimension of each individual fault space, denoted as $\dim(\mathcal{F}(\boldsymbol{\Sigma}_1)+\mathcal{F}(\boldsymbol{\Sigma}_2)) = \dim(\mathcal{F}(\boldsymbol{\Sigma}_1)) = \dim(\mathcal{F}(\boldsymbol{\Sigma}_2))$. Similarly, given g fault spaces of $\boldsymbol{\Sigma}_1, \boldsymbol{\Sigma}_2, \ldots, \boldsymbol{\Sigma}_g$, the sum space of the g fault spaces is the overall space spanned by all the independent fault vectors from all the fault covariance matrices $\boldsymbol{\Sigma}_1, \boldsymbol{\Sigma}_2, \ldots, \boldsymbol{\Sigma}_g$ and it is denoted as $\mathcal{F}(\boldsymbol{\Sigma}_1)+\mathcal{F}(\boldsymbol{\Sigma}_2)+\ldots+\mathcal{F}(\boldsymbol{\Sigma}_g)$. Similarly, we define the intersection $(\mathcal{F}(\boldsymbol{\Sigma}_1) \cap \mathcal{F}(\boldsymbol{\Sigma}_2))$ of two fault spaces as the linear space of $\{\mathbf{v}\colon \mathbf{v} \in \mathcal{F}(\boldsymbol{\Sigma}_1) \text{ and } \mathbf{v} \in \mathcal{F}(\boldsymbol{\Sigma}_2)\}$, the relative complements $(\mathcal{F}(\boldsymbol{\Sigma}_1) \sim \mathcal{F}(\boldsymbol{\Sigma}_2))$ as the linear space such that $(\mathcal{F}(\boldsymbol{\Sigma}_1) \sim \mathcal{F}(\boldsymbol{\Sigma}_2)) \oplus (\mathcal{F}(\boldsymbol{\Sigma}_1) \cap \mathcal{F}(\boldsymbol{\Sigma}_2)) = \mathcal{F}(\boldsymbol{\Sigma}_1)$, where "$\oplus$" represents direct sum of two linear spaces.
- *Fault labels and fault set*. To simplify the notation, we use natural numbers (1, 2, 3, ...) to label all the identified independent faults. If the fault vector of a given fault label, say $\mathbf{v}$, belongs to a fault space $\mathcal{F}(\boldsymbol{\Sigma}_{\mathbf{y}})$, then we say that $\mathbf{v}$ is contained in $\boldsymbol{\Sigma}_{\mathbf{y}}$, denoted as $\mathbf{v} \in \mathcal{F}(\boldsymbol{\Sigma}_{\mathbf{y}})$. A fault set of a fault covariance matrix $\boldsymbol{\Sigma}_{\mathbf{y}}$ is a set of all the fault labels that are contained in $\boldsymbol{\Sigma}_{\mathbf{y}}$. A fault library is a collection of all the historical fault covariance matrices and corresponding fault sets. The size of a fault set is the total number of fault labels that are contained in the fault set. Because fault vectors associated with different faults are independent from one another, it is obvious that the size of a fault set is equal to the dimension of the corresponding fault space.

The various concepts introduced above can be used to study the relationships among fault spaces associated with multiple fault-covariance matrices. However, in practice, the population covariance-matrix of quality measurements is not available. Systematic statistical testing needs to be used to identify the properties of the fault spaces using the corresponding sample covariance matrices.

The Akaike Information Criteria (AIC) and minimum description length (MDL) information criteria can be used to estimate the number of faults in a single fault space $\mathcal{F}(\mathbf{\Sigma_y})$ (Apley and Shi, 2001). The AIC and MDL criteria are given as:

$$\mathrm{AIC}(l) = N(m-l)\log(a_l/g_l) + l(2m-l), \quad (3)$$

and

$$\mathrm{MDL}(l) = N(m-l)\log(a_l/g_l) + l(2m-l)\log(N)/2, \quad (4)$$

where N is the sample size, m is the dimension of the quality measurement, and a_l and g_l are the arithmetic mean and the geometric mean of the $(m-l)$ smallest eigenvalues of sample covariance matrix $\mathbf{S_y}$, respectively. To use this criteria, AIC(l) and MDL(l) are evaluated for $l = 0 \dots m-1$. The estimated fault number k is chosen as the l that minimizes AIC(l) or MDL(l), respectively.

The focus of this paper is to analyze the relationship among multiple fault spaces and to develop systematic signature construction and matching techniques for variation-source identification based on this relationship.

2.2. *Testing procedure on the number of faults in two or more fault covariance matrices*

It is clear that $\mathcal{F}(\mathbf{\Sigma_y})$ is actually the space spanned by certain eigenvectors of $\mathbf{\Sigma_y}$. Therefore, statistical testing procedures on the properties of the eigenspace of $\mathbf{\Sigma_y}$ can be used to identify the variation sources. Several techniques have been developed for this purpose. Krzanowski (1979, 1982) studied the closeness of two eigenspaces using the principal angle between the eigenvectors from each fault covariance matrix. Raich and Cinar (1995) extended this method by using a similarity factor which is the sum of squares of the cosines of the angles between the model axes. Both methods provide an intuitive geometric understanding of the eigenspace. However, it is difficult to find an explicit distribution for either the principal angle or the similarity factor and thus it is difficult to conduct general statistical inferences based on these two statistics. Flury (1987) proposed a simultaneous method to test the common eigenspace among multiple covariance matrices. However, his method does not require the common eigenspace to relate with the largest eigenvalues and thus the common eigenspace might also contain eigenvectors that are not fault vectors. Hence, this method cannot be used for fault identification. Schott (1988, 1991) presented a testing procedure to estimate the size of the common eigenspace by comparing the first k principal components. This method, if used in fault identification, requires the *same* number of faults to have occurred for all the covariance matrices, which severely limits the application of the testing procedure. Boik (2002) further proposed a more general model which subsumes both Flury's and Schott's models as special cases. However, how to parameterize the model for an arbitrary number of faults with any specified magnitude is still under investigation. In this paper, we will use a test statistic, which is actually an extension of the results of Schott (1999) to study the dimension of the fault space of several fault covariance matrices. The following theorem provides a powerful statistical testing procedure which lays the foundation for the signature construction and matching in this paper.

Theorem 1. *Given g samples of m variables of normally distributed quality measurements, the sample and population covariance matrices of these g samples are* $\mathbf{S}_i$ *and* $\mathbf{\Sigma}_i$ $(i = 1, 2, \dots, g)$, *and* $\dim(\mathcal{F}(\mathbf{\Sigma_y})) = k_i$, *then the test statistic, denoted as* T_s, *for the following hypothesis testing, has an asymptotically chi-squared distribution with* $v_s = (\sum_{i=1}^{g} k_i - s)(m-s)$ *degrees of freedom, where*:

$$T_s = n\mathbf{v}_*'(\mathbf{F}\hat{\mathbf{\Phi}}_*\mathbf{F})^+\mathbf{v}_*. \quad (5)$$

The hypothesis testing is:

H_{0s}: $\dim(\mathcal{F}(\mathbf{\Sigma}_1)+\mathcal{F}(\mathbf{\Sigma}_2)+\dots+\mathcal{F}(\mathbf{\Sigma}_g)) = s$ *where* $\max(k_i) - 1 < s < t$ *and* $t = \min(\sum_{i=1}^{g} k_i, m)$
H_{1s}: $\dim(\mathcal{F}(\mathbf{\Sigma}_1)+\mathcal{F}(\mathbf{\Sigma}_2)+\dots+\mathcal{F}(\mathbf{\Sigma}_g)) > s$.

The expression of T_s *is quite complicated. The terms involved in Equation* (5) *are explained as follows*:

- $n = n_1 + \cdots + n_g$, *where* $n_i = N_i - 1$ *and* N_i *is the sample size of the ith sample*, $i = 1, 2, \dots, g$.
- *Let* $\lambda_{i1} \geq \cdots \geq \lambda_{ik_i} > \lambda_{ik_i+1} \geq \cdots \geq \lambda_{im}$ *be the eigenvalues of* $\mathbf{\Sigma}_i$, *with* $\mathbf{q}_{i1}, \dots, \mathbf{q}_{im}$ *being corresponding orthonormal eigenvectors. The ith group's eigenprojection* $\mathbf{P}_i$ *corresponding to the eigenvalues* $\lambda_{i1} \geq \cdots \geq \lambda_{ik_i}$ *is denoted as* $\mathbf{P}_i = \mathbf{q}_{i1}\mathbf{q}_{i1}' + \cdots + \mathbf{q}_{ik_i}\mathbf{q}_{ik_i}'$. *If* H_{0s} *is true, the matrix* $\mathbf{P} = \mathbf{P}_1 + \dots + \mathbf{P}_g$ *will have a rank of s. If* $\lambda_1 \geq \cdots \geq \lambda_s > \lambda_{s+1} = \dots = \lambda_m = 0$ *are the eigenvalues of* $\mathbf{P}$ *and* $\mathbf{q}_1, \dots, \mathbf{q}_m$ *are corresponding orthonormal eigenvectors.* $\hat{\mathbf{P}}_* = \sum_{j=1}^{s} \hat{\lambda}_j\hat{\mathbf{q}}_j\hat{\mathbf{q}}_j'$ *and* $\hat{\mathbf{P}}_*^+$ *is the Moore-Penrose generalized inverse of* $\hat{\mathbf{P}}_*$. *We denote* $\hat{\mathbf{\Gamma}}_0 = (\hat{\mathbf{q}}_{s+1}, \dots, \hat{\mathbf{q}}_m)$ *and* $\hat{\mathbf{\Gamma}}_i = (\hat{\mathbf{q}}_{i1}, \cdots, \hat{\mathbf{q}}_{ik_i})$:

$$\mathbf{v}_* = (\mathrm{vec}(\hat{\mathbf{\Gamma}}_0'\hat{\mathbf{\Gamma}}_1)', \dots, \mathrm{vec}(\hat{\mathbf{\Gamma}}_0'\hat{\mathbf{\Gamma}}_g)')', \quad (6)$$

  where vec(·) *is a stacking vector operator* (Schott, 1997).
- $\hat{\mathbf{\Phi}}_*$ *is defined as a block diagonal matrix* diag $(\hat{\mathbf{\Psi}}_{*1}, \dots, \hat{\mathbf{\Psi}}_{*g}) + \mathbf{V}$, *where* diag(.) *places its elements along the diagonals sequentially*:

$$\hat{\mathbf{\Psi}}_{*f} = \sum_{j=1}^{k_f}\sum_{l=k_f+1}^{m} \frac{n\hat{\lambda}_{fj}\hat{\lambda}_{fl}}{n_f(\hat{\lambda}_{fj} - \hat{\lambda}_{fl})^2}\mathbf{e}_j\mathbf{e}_j' \otimes \hat{\mathbf{\Gamma}}_0'\hat{\mathbf{q}}_{fl}\hat{\mathbf{q}}_{fl}'\hat{\mathbf{\Gamma}}_0,$$

  where $\mathbf{e}_j$ *denotes the* jth *column of the* $k_f \times k_f$ *identity matrix, and* $\otimes$ *is the direct or Kronecker product. For each* (h,i) $(h = 1, \dots, g$ *and* $i = 1, \dots, g)$ *define the*

$k_h(m-s) \times k_i(m-s)$ matrix as:

$$\mathbf{V}_{hi} = \sum_{f=1}^{g} (\hat{\boldsymbol{\Gamma}}'_h \hat{\mathbf{P}}_*^+ \hat{\boldsymbol{\Gamma}}_f \otimes \mathbf{I}_{m-s}) \hat{\boldsymbol{\Psi}}_{*f} (\hat{\boldsymbol{\Gamma}}'_f \hat{\mathbf{P}}_*^+ \hat{\boldsymbol{\Gamma}}_i \otimes \mathbf{I}_{m-s}) - (\hat{\boldsymbol{\Gamma}}'_h \hat{\mathbf{P}}_*^+ \hat{\boldsymbol{\Gamma}}_i \otimes \mathbf{I}_{m-s}) \hat{\boldsymbol{\Psi}}_{*i} - \hat{\boldsymbol{\Psi}}_{*h} (\hat{\boldsymbol{\Gamma}}'_h \hat{\mathbf{P}}_*^+ \hat{\boldsymbol{\Gamma}}_i \otimes \mathbf{I}_{m-s}) \tag{7}$$

Finally, the matrix $\mathbf{V}$ *is defined as a* $\sum_{i=1}^{g} k_i(m-s) \times \sum_{i=1}^{g} k_i(m-s)$ *partitioned matrix and* $\mathbf{V}_{hi}$ *as its (h,i)th block.*

- *The matrix* $\mathbf{F}$ *is the eigenprojection matrix of* $\hat{\boldsymbol{\Phi}}_*$ *corresponding to its* $(\sum_{i=1}^{g} k_i - s)(m-s)$ *largest eigenvalues.*

Proof. The proof of this theorem is provided in the Appendix. ■

Remark 1. Theorem 1 provides a powerful and rigorous testing procedure for variation-source identification. A straightforward application of Theorem 1 is to check how many faults commonly exist among multiple covariance matrices. Figure 2 illustrates this point.

From Fig. 2, the sum of two fault spaces are separated into three parts, i.e., $\mathcal{F}(\boldsymbol{\Sigma}_1) \sim \mathcal{F}(\boldsymbol{\Sigma}_2)$, $\mathcal{F}(\boldsymbol{\Sigma}_2) \sim \mathcal{F}(\boldsymbol{\Sigma}_1)$, and $\mathcal{F}(\boldsymbol{\Sigma}_1) \cap \mathcal{F}(\boldsymbol{\Sigma}_2)$. From linear algebra, we have that:

$$\dim(\mathcal{F}(\boldsymbol{\Sigma}_1) + \mathcal{F}(\boldsymbol{\Sigma}_2)) = \dim(\mathcal{F}(\boldsymbol{\Sigma}_1)) + \dim(\mathcal{F}(\boldsymbol{\Sigma}_2)) - \dim(\mathcal{F}(\boldsymbol{\Sigma}_1) \cap \mathcal{F}(\boldsymbol{\Sigma}_2)). \tag{8}$$

Using Theorem 1, we can easily obtain $\dim(\mathcal{F}(\boldsymbol{\Sigma}_1) \cap \mathcal{F}(\boldsymbol{\Sigma}_2))$. For example, assume that there are two covariance matrices $\boldsymbol{\Sigma}_1$ and $\boldsymbol{\Sigma}_2$ and $\dim(\mathcal{F}(\boldsymbol{\Sigma}_1))$ and $\dim(\mathcal{F}(\boldsymbol{\Sigma}_2))$ are both two from the MDL testing criteria (Equation (4)) based on the sample covariance matrices $\mathbf{S}_1$ and $\mathbf{S}_2$. Then we can select s as two and three to conduct the hypothesis testing of H_{0s}: $\dim(\mathcal{F}(\boldsymbol{\Sigma}_1) + \mathcal{F}(\boldsymbol{\Sigma}_2)) = s$ using the test statistic T_s. First, the value of T_s can be calculated according to Equation (5). Then T_s is compared with the critical value of the test, $\chi^2_{1-\alpha,\upsilon_s}$, where α is a selected significance level such as 0.05, 0.01, etc. If T_s is larger than the critical value, then we claim that there is significant statistical evidence against H_{0s} and we have to reject H_{0s}. Otherwise we claim that there is no significant evidence against H_{0s} and we have to accept $\dim(\mathcal{F}(\boldsymbol{\Sigma}_1) + \mathcal{F}(\boldsymbol{\Sigma}_2))$ as s. Finally, the minimum of the values of s that satisfy $T_s < \chi^2_{1-\alpha,\upsilon_s}$ will be taken as the estimated dimension of $\dim(\mathcal{F}(\boldsymbol{\Sigma}_1) + \mathcal{F}(\boldsymbol{\Sigma}_2))$. The testing result is very informative from a variation-source identification point of view. In the current example, if the testing indicates that $s = 2$, then we can claim that the same faults happen in the first and second samples. Similarly, if $s = 3$, then there is only one and if $s = 4$, then no common faults happen in the two samples, respectively.

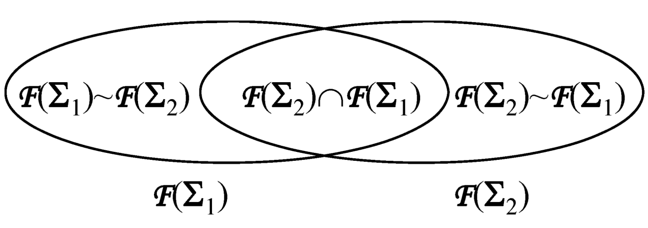

Fig. 2. The relationship between two fault spaces.

From the above discussion of the application of Theorem 1, it is clear that a sample covariance matrix $\mathbf{S}_1$ can be used as the *signature* of the fault that happens during the sampling period. When a new sample ($\mathbf{S}_2$) is obtained, we can simply check whether or not $\dim(\mathcal{F}(\boldsymbol{\Sigma}_1) + \mathcal{F}(\boldsymbol{\Sigma}_2))$ is larger than $\mathcal{F}(\boldsymbol{\Sigma}_2)$. If it is not larger, then the same fault represented by $\mathbf{S}_1$ happened in the second sample. Because it is reasonable to assume that people have understood previously identified faults, this technique can help tremendously in fault identification and elimination.

Because the testing procedure provided by Theorem 1 can be applied to multiple-fault conditions, the fault signature for simultaneous multiple faults can be obtained. Furthermore, by considering multiple sample-covariance matrices together, more complicated fault signatures can be achieved. This can help to extract more information from the measurement data and thus fully utilize the existing measurement data. In the next section, we will present the construction of three types of fault signatures.

2.3. *Construction of fault signatures*

The purpose of a fault signature is to pinpoint a particular fault set whenever it happens again. In order to fully utilize the existing samples and their covariance matrices under a fault condition, we propose three types of fault signatures: type-A, type-B, and type-C. The reason that we classify the fault signatures into three types is because we have to apply different testing procedures for each type of fault signature in order to successfully identify the fault in the new samples.

2.3.1. *The type-A fault signature*

The type-A fault signature is simple: any historical fault covariance matrix can be chosen as the type-A fault signature for the fault set associated with it. We denote $< \mathbf{S}_1, \mathbf{A} >$ or $< \mathbf{S}_1 >$ as the type-A fault signature of the faults contained in $\mathcal{F}(\boldsymbol{\Sigma}_1)$. The utilization of a type-A fault is described by Proposition 1.

Proposition 1. *Given a type-A fault signature* $\mathbf{S}_0$ *(the corresponding population covariance being* $\boldsymbol{\Sigma}_0$*) that contains k faults and a new sample with sample covariance* $\mathbf{S}_1$ *(the corresponding population covariance being* $\boldsymbol{\Sigma}_1$*), then* $\mathcal{F}(\boldsymbol{\Sigma}_0) \subseteq \mathcal{F}(\boldsymbol{\Sigma}_1)$ *if and only if* $\dim(\mathcal{F}(\boldsymbol{\Sigma}_0) \cap \mathcal{F}(\boldsymbol{\Sigma}_1)) = \dim(\mathcal{F}(\boldsymbol{\Sigma}_0))$.

Proof. The proof of this proposition is quite straightforward and is omitted here. ■

The value of $\dim(\mathcal{F}(\boldsymbol{\Sigma}_0) \cap \mathcal{F}(\boldsymbol{\Sigma}_1))$ can be determined using Theorem 1. This proposition provides us with a procedure to utilize the type-A signature to test if all the faults in $\mathcal{F}(\boldsymbol{\Sigma}_0)$ occur in the new sample. The type-A fault signature has the simplest testing procedure. Hence, we recommend the type-A fault signature as the first choice.

2.3.2. *Type-B fault signature*

Type-A fault signatures provide a simple testing procedure for fault identification. However, we may not always be able to obtain a type-A fault signature for an individual fault because some faults may have limited occurrences and historically they may always occur simultaneously with some other faults. In this case, we need to investigate the interactions among multiple covariance matrices to obtain fault signatures for those faults.

From Fig. 2, we have that:

$$\mathcal{F}(\mathbf{\Sigma}_1)+\mathcal{F}(\mathbf{\Sigma}_2)=\mathcal{F}(\mathbf{\Sigma}_1)\sim\mathcal{F}(\mathbf{\Sigma}_2)+\mathcal{F}(\mathbf{\Sigma}_2)\sim\mathcal{F}(\mathbf{\Sigma}_1)+\mathcal{F}(\mathbf{\Sigma}_1)\cap\mathcal{F}(\mathbf{\Sigma}_2). \quad (9)$$

We denote $<\mathbf{S}_1, \mathbf{S}_2, \mathbf{B}>$ as the type-B fault signature of the faults contained in $\mathcal{F}(\mathbf{\Sigma}_1)\cap\mathcal{F}(\mathbf{\Sigma}_2)$.

Proposition 2. *Given two sample covariance matrices* $\mathbf{S}_1$ *and* $\mathbf{S}_2$, *and denoting the corresponding population covariance as* $\mathbf{\Sigma}_1$ *and* $\mathbf{\Sigma}_2$, *respectively*, *then for any new covariance matrix* $\mathbf{S}_i$ (*the corresponding population covariance being* $\mathbf{\Sigma}_i$), *we have* $\mathcal{F}(\mathbf{\Sigma}_1)\cap\mathcal{F}(\mathbf{\Sigma}_2)\subseteq\mathcal{F}(\mathbf{\Sigma}_i)$ *if and only if* $\dim(\mathcal{F}(\mathbf{\Sigma}_1)\cap\mathcal{F}(\mathbf{\Sigma}_i))+\dim(\mathcal{F}(\mathbf{\Sigma}_2)\cap\mathcal{F}(\mathbf{\Sigma}_i))=k_0+\dim(\mathcal{F}(\mathbf{\Sigma}_1)\cap\mathcal{F}(\mathbf{\Sigma}_2))$ *where*:

$$k_0=\dim(\mathcal{F}(\mathbf{\Sigma}_i))-[\dim(\mathcal{F}(\mathbf{\Sigma}_i)+\mathcal{F}(\mathbf{\Sigma}_1)+\mathcal{F}(\mathbf{\Sigma}_2))-\dim(\mathcal{F}(\mathbf{\Sigma}_1)+\mathcal{F}(\mathbf{\Sigma}_2))] \quad (10)$$

Physically, k_0 *represents the number of common faults between* $\mathcal{F}(\mathbf{\Sigma}_i)$ *and* $\mathcal{F}(\mathbf{\Sigma}_1)+\mathcal{F}(\mathbf{\Sigma}_2)$.

Proof. First, denote the number of common faults between $\mathcal{F}(\mathbf{\Sigma}_1)$ and $\mathcal{F}(\mathbf{\Sigma}_2)$ as CF, i.e., $CF=\dim(\mathcal{F}(\mathbf{\Sigma}_1)\cap\mathcal{F}(\mathbf{\Sigma}_2))$, we have that:

$$\dim(\mathcal{F}(\mathbf{\Sigma}_1)\cap\mathcal{F}(\mathbf{\Sigma}_i))+\dim(\mathcal{F}(\mathbf{\Sigma}_2)\cap\mathcal{F}(\mathbf{\Sigma}_i))-k_0-CF=0 \quad (11)$$

then substituting Equation (10) into Equation (11) and noticing (8) and that $\dim(\mathcal{F}(\mathbf{\Sigma}_1)+\mathcal{F}(\mathbf{\Sigma}_i))+\dim(\mathcal{F}(\mathbf{\Sigma}_2)+\mathcal{F}(\mathbf{\Sigma}_i))=\dim(\mathcal{F}(\mathbf{\Sigma}_1)+\mathcal{F}(\mathbf{\Sigma}_2)+\mathcal{F}(\mathbf{\Sigma}_i))+\dim((\mathcal{F}(\mathbf{\Sigma}_1)\cap\mathcal{F}(\mathbf{\Sigma}_2))+\mathcal{F}(\mathbf{\Sigma}_i))$, we have that $\dim(\mathcal{F}(\mathbf{\Sigma}_i))-\dim((\mathcal{F}(\mathbf{\Sigma}_1)\cap\mathcal{F}(\mathbf{\Sigma}_2))+\mathcal{F}(\mathbf{\Sigma}_i))=0$. Therefore, $\dim(\mathcal{F}(\mathbf{\Sigma}_i))=\dim((\mathcal{F}(\mathbf{\Sigma}_1)\cap\mathcal{F}(\mathbf{\Sigma}_2))+\mathcal{F}(\mathbf{\Sigma}_i))$ and thus we have that $\mathcal{F}(\mathbf{\Sigma}_1)\cap\mathcal{F}(\mathbf{\Sigma}_2)\subseteq\mathcal{F}(\mathbf{\Sigma}_i)$.

Second, if $\mathcal{F}(\mathbf{\Sigma}_1)\cap\mathcal{F}(\mathbf{\Sigma}_2)\subseteq\mathcal{F}(\mathbf{\Sigma}_i)$, then $\dim((\mathcal{F}(\mathbf{\Sigma}_1)\cap\mathcal{F}(\mathbf{\Sigma}_2))+\mathcal{F}(\mathbf{\Sigma}_i))=\dim(\mathcal{F}(\mathbf{\Sigma}_i))$ and Equation (11) can be simply obtained.

The geometric interpretation of Proposition 2 is illustrated in Fig. 3. Each oval in the figure represents one fault space. The intersection between $F(\mathbf{\Sigma}_i)$ and $\mathcal{F}(\mathbf{\Sigma}_1)+\mathcal{F}(\mathbf{\Sigma}_2)$ are represented by three spaces: (i) $\mathbf{F}_1=(\mathcal{F}(\mathbf{\Sigma}_1)\cap\mathcal{F}(\mathbf{\Sigma}_i))\sim\mathcal{F}(\mathbf{\Sigma}_2)$, (ii) $\mathbf{F}_2=(\mathcal{F}(\mathbf{\Sigma}_2)\cap\mathcal{F}(\mathbf{\Sigma}_i))\sim\mathcal{F}(\mathbf{\Sigma}_1)$, and (iii) $\mathbf{F}_3=\mathcal{F}(\mathbf{\Sigma}_1)\cap\mathcal{F}(\mathbf{\Sigma}_2)\cap\mathcal{F}(\mathbf{\Sigma}_i)$. If Equation (11) holds, $\mathbf{F}_3$ will completely fall inside $\mathcal{F}(\mathbf{\Sigma}_i)$. Therefore,

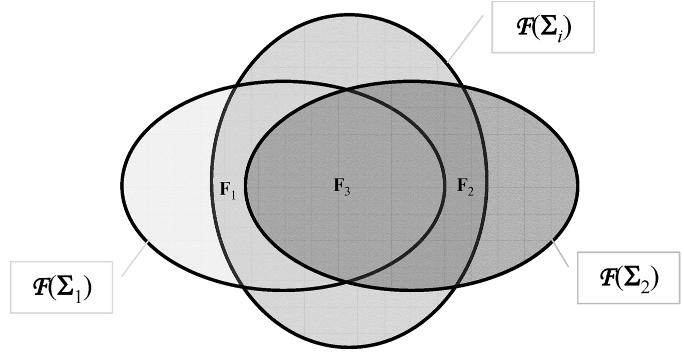

Fig. 3. Geometric interpretation of Proposition 2.

then $<\mathbf{S}_1, \mathbf{S}_2, \mathbf{B}>$ can be viewed as a signature of the faults contained in $\mathbf{F}_3$.

This proposition provides a procedure to test if the intersection of two fault spaces has happened in the newly collected samples ($\mathbf{S}_i$) by checking whether Equation (11) is valid using the testing of Theorem 1. ■

2.3.3. *Type-C fault signature*

Similar to the definition of type-B fault signature, we define $<\mathbf{S}_1, \mathbf{S}_2, \mathbf{C}>$ as the type-C fault signature of the faults contained in $\mathcal{F}(\mathbf{\Sigma}_1)\sim\mathcal{F}(\mathbf{\Sigma}_2)$. The utilization of a type-C signature is described by Proposition 3.

Proposition 3. *Given two sample covariance matrices* $\mathbf{S}_1$ *and* $\mathbf{S}_2$, *and denoting the corresponding population covariance as* $\mathbf{\Sigma}_1$ *and* $\mathbf{\Sigma}_2$, *respectively*, *then for any new covariance matrix* $\mathbf{S}_i$ (*the corresponding population covariance being* $\mathbf{\Sigma}_i$), *we have that* $\mathcal{F}(\mathbf{\Sigma}_1)\sim\mathcal{F}(\mathbf{\Sigma}_2)\subseteq\mathcal{F}(\mathbf{\Sigma}_i)$ *if and only if*

$$\dim(\mathcal{F}(\mathbf{\Sigma}_2)\cap\mathcal{F}(\mathbf{\Sigma}_i))+\dim(\mathcal{F}(\mathbf{\Sigma}_1)\sim\mathcal{F}(\mathbf{\Sigma}_2))=k_0. \quad (12)$$

Proof. First, we denote $UF=\dim(\mathcal{F}(\mathbf{\Sigma}_1)\sim\mathcal{F}(\mathbf{\Sigma}_2))$ as the number of unique faults in $\mathcal{F}(\mathbf{\Sigma}_1)$ but not in $\mathcal{F}(\mathbf{\Sigma}_2)$) and substitute Equation (10) into Equation (12). Noticing that $\dim(\mathcal{F}(\mathbf{\Sigma}_2)\cap\mathcal{F}(\mathbf{\Sigma}_i))=\dim(\mathcal{F}(\mathbf{\Sigma}_2))+\dim(\mathcal{F}(\mathbf{\Sigma}_i))-\dim(\mathcal{F}(\mathbf{\Sigma}_2)+\mathcal{F}(\mathbf{\Sigma}_i))$ and $\dim(\mathcal{F}(\mathbf{\Sigma}_1)\sim\mathcal{F}(\mathbf{\Sigma}_2))+\dim(\mathcal{F}(\mathbf{\Sigma}_2))=\dim(\mathcal{F}(\mathbf{\Sigma}_2)+\mathcal{F}(\mathbf{\Sigma}_1))$, we have that $\dim(\mathcal{F}(\mathbf{\Sigma}_i)+\mathcal{F}(\mathbf{\Sigma}_1)+\mathcal{F}(\mathbf{\Sigma}_2))=\dim(\mathcal{F}(\mathbf{\Sigma}_2)+\mathcal{F}(\mathbf{\Sigma}_i))$.

Therefore, $\mathcal{F}(\mathbf{\Sigma}_1)\subseteq\mathcal{F}(\mathbf{\Sigma}_2)+\mathcal{F}(\mathbf{\Sigma}_i)\Rightarrow\mathcal{F}(\mathbf{\Sigma}_1)\sim(\mathcal{F}(\mathbf{\Sigma}_2)\subseteq(\mathcal{F}(\mathbf{\Sigma}_i)+\mathcal{F}(\mathbf{\Sigma}_2))\sim\mathcal{F}(\mathbf{\Sigma}_2)$, however, because $(\mathcal{F}(\mathbf{\Sigma}_i)+\mathcal{F}(\mathbf{\Sigma}_2))\sim\mathcal{F}(\mathbf{\Sigma}_2)=(\mathcal{F}(\mathbf{\Sigma}_i)\sim\mathcal{F}(\mathbf{\Sigma}_2))$ and $(\mathcal{F}(\mathbf{\Sigma}_i)\sim\mathcal{F}(\mathbf{\Sigma}_2))\subseteq\mathcal{F}(\mathbf{\Sigma}_i)$, we have $\mathcal{F}(\mathbf{\Sigma}_1)\sim\mathcal{F}(\mathbf{\Sigma}_2)\subseteq\mathcal{F}(\mathbf{\Sigma}_i)$.

Second, if $(\mathcal{F}(\mathbf{\Sigma}_1)\sim\mathcal{F}(\mathbf{\Sigma}_2))\subseteq\mathcal{F}(\mathbf{\Sigma}_i)$, then we have that $\mathcal{F}(\mathbf{\Sigma}_1)+\mathcal{F}(\mathbf{\Sigma}_2)+\mathcal{F}(\mathbf{\Sigma}_i)=\mathcal{F}(\mathbf{\Sigma}_2)+\mathcal{F}(\mathbf{\Sigma}_i)$ and thus Equation (12) can be obtained through a straightforward derivation. ■

The geometric interpretation of Proposition 3 is shown in Fig. 4. Similar to the interpretation of Proposition 2, the intersection between $\mathcal{F}(\mathbf{\Sigma}_i)$ and $\mathcal{F}(\mathbf{\Sigma}_1)+\mathcal{F}(\mathbf{\Sigma}_2)$ consists of three spaces: $\mathbf{F}_1$, $\mathbf{F}_2$, and $\mathbf{F}_3$. If Equation (12) holds, then $\mathbf{F}_1$

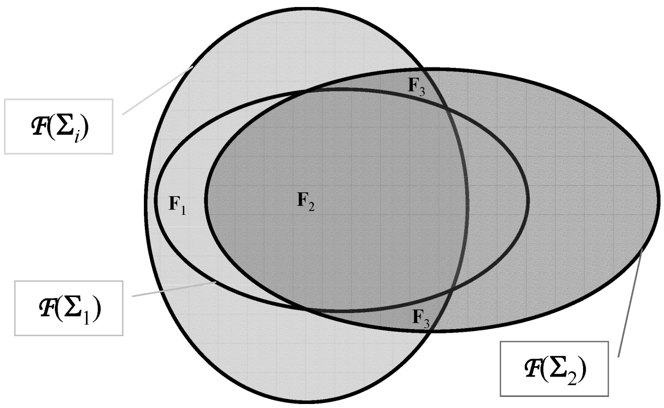

Fig. 4. Geometric interpretation of Proposition 3.

will fall completely inside $\mathcal{F}(\boldsymbol{\Sigma}_i)$. Therefore, $<\mathbf{S}_1, \mathbf{S}_2, \mathbf{C}>$ can be used as a signature of $\mathcal{F}(\boldsymbol{\Sigma}_1)\sim\mathcal{F}(\boldsymbol{\Sigma}_2)$.

This proposition provides a procedure to test if the complement part of two fault spaces $\mathcal{F}(\boldsymbol{\Sigma}_1) \sim \mathcal{F}(\boldsymbol{\Sigma}_2)$ has happened in the newly collected samples ($\mathbf{S}_i$) by checking whether Equation (12) is valid using the testing of Theorem 1 and the signature of $<\mathbf{S}_1, \mathbf{S}_2, \mathbf{C}>$. The value of $\dim(\mathcal{F}(\boldsymbol{\Sigma}_1) \sim \mathcal{F}(\boldsymbol{\Sigma}_2))$ can be estimated through the identity $\dim(\mathcal{F}(\boldsymbol{\Sigma}_1) \sim \mathcal{F}(\boldsymbol{\Sigma}_2)) = \dim(\mathcal{F}(\boldsymbol{\Sigma}_1)) - \dim(\mathcal{F}(\boldsymbol{\Sigma}_1) \cap \mathcal{F}(\boldsymbol{\Sigma}_2))$, where $\dim(\mathcal{F}(\boldsymbol{\Sigma}_1))$ can be determined using MDL criteria and $\dim(\mathcal{F}(\boldsymbol{\Sigma}_1) \cap \mathcal{F}(\boldsymbol{\Sigma}_2))$ can be determined by Equation (8) and Theorem 1.

The construction of the fault signatures should be based on the requirement of engineering applications. In many applications, we want to isolate individual variation sources. Hence, the signature of a single fault has the highest priority for construction. However, the signatures of multiple faults set can also be constructed following the same procedure. The fault signatures can be constructed in the following one, two or three steps depending on the available information.

Step 1. For each fault label, search for the type-A fault signature for this particular fault. If we can find a fault covariance matrix that contains only the given fault, we will assign this fault covariance matrix as the type-A fault signature of this particular fault and stop the search for the fault signature of this fault.

Step 2. If a type-A fault signature cannot be found, we extend the search scope to test if one fault set that contains this fault label and another fault set that does not contain this fault label are able to generate a type-C signature for this particular fault. If found, we will stop the search to the signature of this particular fault.

Step 3. If a type-C fault signature of this particular fault still cannot be found, we further extend the search scope to test if any two fault sets that contain this fault label are able to generate a type-B signature for this particular fault. If a type-B fault signature still cannot be found, then this fault always occurs simultaneously with some other faults and cannot be uniquely detected by the available data. In this case, a fault signature for multiple faults that contains this fault label is recommended to be constructed.

Remark 2. In this procedure, we prefer a type-C fault signature to a type-B fault signature because the testing procedure for type-C fault signatures generally has a smaller type-I error than that of the type-B fault signature. This result can be observed in Section 2.5.

Remark 3. The proposed signature-construction procedure only involves two covariance matrices at most. Theoretically, we might obtain even more detailed partitions based on three or more covariance matrices. However, in many cases, this is not necessary because: (i) further partitions will significantly increase the complexity of the testing procedure and thus make the procedure less effective in practice; and (ii) due to the improved technologies currently in use in most engineering applications, it is very rare that many faults (more than six) will happen simultaneously. Hence, most historical fault sets will contain a relatively smaller number of faults which can be handled more efficiently by the fault signatures based on two fault spaces only.

2.4. *The procedures for signature construction and variation-source identification*

Based on the rigorous testing procedure for signature matching presented in Section 2.2 and the various signature-construction methods presented in Section 2.3, systematic variation-source identification can be achieved. The basic steps are summarized in Fig. 5.

Step 1. The multivariate product-quality measurements are obtained in the data collection step. The sample size is assumed to be N and the dimension of the measurement is m.

Step 2. Based on the quality measurement, we can calculate the sample covariance matrix. From this covariance matrix, the number of significant variation sources can be estimated and tested by the AIC or MDL criteria introduced in Section 2.1.

Step 3. By matching each fault signature in the fault library with the new fault covariance matrix, we can determine the variation sources associated with the new fault covariance matrix. The testing is based on Theorem 1 and the three propositions in Section 2.3. If no match is found, we must assume that new variation sources have been found.

Step 4. Two parts are added to the fault library in an update procedure: the fault covariance matrix and its corresponding fault set identified in Step 3.

Step 5. After we obtain the new fault covariance matrix and its fault set, we might want to utilize the new information. From the different type of variation sources of interest we construct fault signatures for

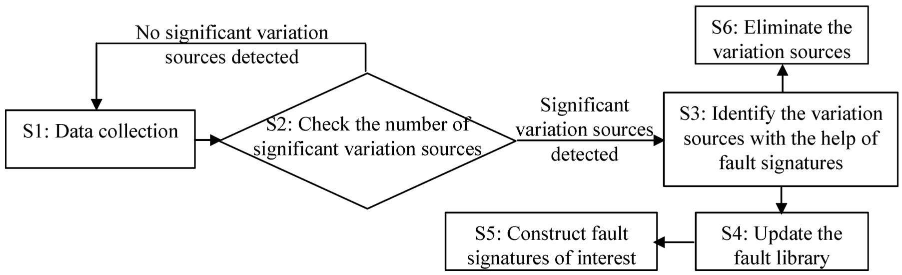

Fig. 5. The procedure of variation-source identification.

the new faults or even some new combinations of historically identified faults. The method for the construction of fault signatures was introduced in Section 2.3.

Step 6. After the variation sources are identified, we relate the fault directions with the process variables and attempt to eventually eliminate the variation sources.

2.5. *The false alarm rate of the procedure*

There are two stages for the identification of variation sources: fault detection and fault diagnosis. The procedure introduced in Section 2.4 includes both fault detection and fault diagnosis. To evaluate the performance of this method, we studied the false alarm rate for both of them.

In fault detection, the false alarm rate is the probability that our method will falsely claim that at least one fault occurred when the system is actually under normal working condition (no fault occurred). In our proposed procedure, this false alarm rate is related with the MDL test only. If the MDL test falsely identified a fault which actually does not exist, then this is a false alarm. A Monte Carlo simulation was used to evaluate this false alarm rate. We used the linear model $\mathbf{y} = \mathbf{A}\mathbf{f} + \boldsymbol{\varepsilon}$ to generate the sample covariance matrices and used the MDL test to estimate the number of faults in the system. A typical parameter setting in practice was selected in the simulation: the maximal number of faults in the system was five faults; the dimension of $\mathbf{y}$ was ten; we also assumed a variance of the noise as $\sigma_\varepsilon^2 = 0.01^2$ and all the eigenvalues of $\boldsymbol{\Sigma}_\mathbf{f}$ to be equal to 0.005^2, which corresponds to the situation when no fault has occurred in the system. Without loss of generality, we also assumed that all the columns of matrix $\mathbf{A}$ are orthogonal to one another. In total, 10 000 cases were simulated. For a sample size of $N = 50$, the false alarm rate was equal to a very small value, 0.0005, which shows that the MDL test is quite effective in fault detection.

In fault diagnosis, we already know there are fault(s) in the new sample and that the false alarm rate or type-I error is defined as the probability of incorrectly identifying the existing fault(s). The overall type-I error of the diagnosis includes both the errors in the MDL tests (the probability that we falsely estimate the total number of faults in the system) and the errors in the hypothesis testing for fault signature matching (the probability that we did not correctly identify the fault when the fault actually occurred). It is very difficult to obtain analytical results on the overall type-I error. To demonstrate the effectiveness of the proposed procedure, Monte Carlo simulation was again used. The parameter setting used here is the same as that used in the previous fault detection case except that an extra parameter $\boldsymbol{\sigma}_\mathbf{p}^2/\sigma_\varepsilon^2$ was specified, where $\boldsymbol{\sigma}_\mathbf{p}^2$ is the variance of the occurring process fault. It is easy to understand that a larger value of $\boldsymbol{\sigma}_\mathbf{p}^2/\sigma_\varepsilon^2$ will differentiate the fault from the noise better and thus give a smaller type-I error of the hypothesis test. Hence, we denote $SNR \equiv \boldsymbol{\sigma}_\mathbf{p}^2/\sigma_\varepsilon^2$ as an important factor in the simulation. Intuitively, the value of SNR can be viewed as the signal to noise ratio in the system. For the sake of simplification, we also assumed that all the sample covariance matrices and the fault signature matrices share the sample size N and SNR in each case. However, this is not a limitation of the testing procedure. In total, 5000 cases were simulated for each type of fault signature. Assuming that the fault covariance matrix $\mathbf{S}_0$ is the signature matrix of fault $\{1\}$, fault covariance matrix $\mathbf{S}_1$ is the signature matrix of fault $\{1,2\}$, fault covariance matrix $\mathbf{S}_2$ is the signature matrix of $\{1,3\}$, and fault covariance matrix $\mathbf{S}_3$ is the signature matrix of fault $\{2\}$, we have $<\mathbf{S}_0, \mathbf{A}>$, $<\mathbf{S}_1, \mathbf{S}_2, \mathbf{B}>$ and $<\mathbf{S}_1, \mathbf{S}_3, \mathbf{C}>$ as the type-A signature, type-B signature and type-C signature of fault $\{1\}$, respectively. For the type-A signature, we generated a new covariance matrix $\mathbf{S}_{\text{new}}$ that contained fault $\{1,2\}$. If the testing procedure cannot correctly estimate the number of faults in $\mathbf{S}_0$ and $\mathbf{S}_{\text{new}}$ or cannot correctly identify that $\mathbf{S}_{\text{new}}$ contains fault $\{1\}$, then it will be marked as an error case. The false alarm rate for the testing procedure of this type-A signature is calculated by the total number of error cases divided by 5000. Similarly, the new covariance matrices $\mathbf{S}_{\text{new}}$ for type-B and type-C signatures are the covariance matrices that contain faults $\{1\}$ and $\{1,3\}$ respectively. The false alarm rate for each type of fault signature is presented in Table 1.

Remark 4. In general, the false alarm rates of the testing procedures are: type-A fault signature $<$ type-C fault signature $<$ type-B fault signature. This result is reasonable because more hypothesis tests are used for type-B fault signature matching.

Table 1. False alarm rate for each type of fault signature in the simulation

			α				
Signature type	*N*	*SNR*	$\alpha_I = 0.01$	$\alpha_I = 0.02$	$\alpha_I = 0.03$	$\alpha_I = 0.04$	$\alpha_I = 0.05$
A	50	10	0.437	0.456	0.469	0.480	0.491
		20	0.051	0.069	0.086	0.106	0.119
		50	0.039	0.059	0.077	0.092	0.108
	100	10	0.060	0.074	0.090	0.105	0.121
		20	0.022	0.043	0.059	0.074	0.084
		50	0.026	0.040	0.056	0.070	0.081
	200	10	0.019	0.030	0.042	0.057	0.070
		20	0.017	0.031	0.043	0.054	0.064
		50	0.013	0.026	0.040	0.052	0.060
B	50	10	0.699	0.716	0.734	0.747	0.759
		20	0.113	0.158	0.192	0.222	0.250
		50	0.092	0.134	0.174	0.201	0.230
	100	10	0.120	0.161	0.190	0.216	0.241
		20	0.058	0.090	0.123	0.147	0.176
		50	0.049	0.086	0.116	0.143	0.170
	200	10	0.044	0.076	0.103	0.127	0.149
		20	0.036	0.063	0.085	0.108	0.134
		50	0.033	0.060	0.087	0.115	0.138
C	50	10	0.663	0.673	0.683	0.691	0.697
		20	0.061	0.083	0.102	0.123	0.137
		50	0.045	0.064	0.084	0.100	0.117
	100	10	0.081	0.098	0.112	0.124	0.135
		20	0.022	0.037	0.050	0.061	0.073
		50	0.021	0.036	0.048	0.063	0.075
	200	10	0.018	0.033	0.048	0.062	0.075
		20	0.019	0.029	0.041	0.053	0.065
		50	0.018	0.029	0.040	0.054	0.066

*α_1 is the type-I error specified on the hypothesis test in Theorem 1.

Remark 5. As the sample size N increases the false alarm rate decreases, which is consistent with the intuitive understanding that we are more confident in identifying the faults given more information about the data.

Remark 6. When the fault magnitude (represented by the SNR value given in the table) is small ($SNR < 50$ in this case), a larger fault magnitude generally will have a smaller false alarm rate in the fault diagnosis. This is also reasonable since a larger SNR value tends to differentiate a fault from the noise. However, if the fault magnitude becomes very large ($SNR > 50$ in this case), it may not have much influence on the false alarm rate.

Remark 7. For $SNR = 10$ and $N = 50$, the false alarm rate presented in the table is very large which makes the proposed procedure ineffective. From a close examination of the simulation results, we found that the type-I error for the proposed hypothesis test is still very small whereas the type-I error of the MDL test contributes to more than 90% of the large false alarm rate. Hence, we should avoid a small sample size when the fault magnitude is not very large. If an alternative test to the MDL test can be found that is able to provide a more reliable estimate of the number of faults, the proposed procedure in this particular case can still be used. This is an area of future research.

It should be pointed out that it is unsafe to draw very general conclusions from one simulation case. However, because the simulation is a typical case in practice, it is reasonable to conclude that the proposed method is an effective method in many engineering applications. Furthermore, as a rule of thumb for most practical situations, when $SNR > 20$ or the sample size is ten times the dimension of $\mathbf{y}$ (in this simulation case $N > 100$), the proposed method has a good performance.

In the next section, a comprehensive case study is presented to illustrate the utilization of the proposed technique.

3. Case study

3.1. *Introduction to the process*

In this case study, a machining process is adopted to illustrate the effectiveness of our proposed method. To machine a workpiece, we need first to locate the workpiece in a fixture system and then mount the fixture system on the working table of the machining center. The position of the cutting

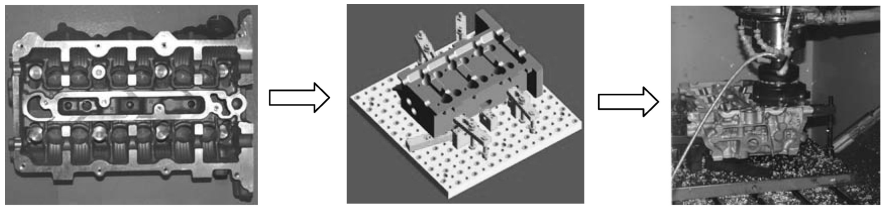

(a) (b) (c)

Fig. 6. Illustration of a machining process: (a) the workpiece; (b) the fixture system; and (c) the machining operation.

tool during cutting is calibrated with respect to the working table. The process is shown in Fig. 6(a–c).

In Fig. 6(a–c), the workpiece is an automotive engine component, the fixture system is of 3-2-1 configuration, and the machine tool is a vertical machining center (only the cutting tool and the working table of this machining center are shown in the figure). The 3-2-1 fixturing setup is widely used in practice, in which there are $3 + 2 + 1 = 6$ locating pins. The position and orientation of the workpiece is fixed in space with respect to the fixture if the workpiece touches these six pins.

is a 31 by 1 vector that represents the measurement noise. A CMM is the most common device in practice. Based on the normal accuracy of a CMM, we select $\sigma_\varepsilon = 0.01$ mm. The process normal variation is around 0.05 mm. Furthermore, for this particular cover face machining operation, $\mathbf{A}$ can be obtained as:

$$\mathbf{A} = \begin{bmatrix} \boldsymbol{\Gamma}_1 \\ \boldsymbol{\Gamma}_2 \end{bmatrix},$$

where

$$\boldsymbol{\Gamma}_1 = [\boldsymbol{\Gamma}_{11}\ \mathbf{0}], \boldsymbol{\Gamma}_2 = [\mathbf{0}\ \boldsymbol{\Gamma}_{22}] \quad \text{and :}$$

$$\boldsymbol{\Gamma}_{11} = \begin{bmatrix} -0.5402 & -0.6455 & -0.2664 & 0.0683 & 0.5158 & 0.8555 & 0.9902 & 1.1863 & 1.3106 & 1.0177 & 0.6394 & 0.3403 & 0.0530 & -0.0820 & -0.2776 \\ 0.9690 & 0.5991 & 0.2203 & -0.1140 & -0.5612 & -0.9005 & -0.7058 & -0.4225 & -0.2428 & 0.1052 & 0.4597 & 0.7585 & 1.0455 & 0.8192 & 0.5367 \\ 0.5711 & 1.0464 & 1.0461 & 1.0458 & 1.0453 & 1.0450 & 0.7156 & 0.2362 & -0.0678 & -0.1229 & -0.0991 & -0.0988 & -0.0985 & 0.2628 & 0.7409 \end{bmatrix}^T,$$

$$\boldsymbol{\Gamma}_{22} = \begin{bmatrix} -0.6349 & -0.4590 & -0.0332 & 0.2510 & 0.6955 & 1.0215 & 1.1372 & 1.1155 & 0.9048 & 0.6472 & 0.5864 & 0.3875 & 0.0777 & -0.1490 & -0.4063 & 0.0776 \\ 0.9602 & 0.6817 & 0.2556 & -0.0288 & -0.4736 & -0.5857 & -0.5031 & -0.3477 & -0.1368 & 0.1210 & -0.0142 & 0.3998 & 0.7098 & 0.9368 & 0.9339 & 0.4496 \\ 0.6747 & 0.7773 & 0.7776 & 0.7778 & 0.7781 & 0.5641 & 0.3659 & 0.2322 & 0.2320 & 0.2318 & 0.4279 & 0.2127 & 0.2124 & 0.2123 & 0.4725 & 0.4728 \end{bmatrix}^T.$$

The cutting tool path is calibrated with respect to the nominal fixturing system. Clearly, an error in the position of the locating pins will cause a geometric error in the machined feature. Because of these location pin errors the position of the workpiece will deviate from its nominal position. However, the cutting tool path is still determined with respect to the nominal location of the workpiece. Eventually, a dimensional error in the workpiece will be induced by the fixture error. By measuring the position and orientation of the resulting workpiece quality, the faulty locating pin can be identified.

For the sake of simplicity, we only consider the identification of locating pin faults of simple machining operations in this case study. The machining operation is illustrated in Fig. 6(c). In this operation, the cover face of the engine component is milled. The joint face of the workpiece will also be milled using this setup. The quality measurements for this operation are the deviations of 31 points on the cover face and joint face from their nominal values. The relationship between the quality measurements and the errors in the locating pins can be described by $\mathbf{y} = \mathbf{A}\mathbf{f} + \boldsymbol{\varepsilon}$. In this model, $\mathbf{y}$ is a 31 by 1 vector that includes the measurement of 31 points. $\mathbf{y}$ is in the units of millimeters. $\mathbf{f}$ is a 6 by 1 vector that represents the error in the six locating pins of the fixturing system used for cover and joint face milling. $\boldsymbol{\varepsilon}$

Please note that the columns of $\mathbf{A}$ have not been normalized. This model is validated in Zhou *et al.* (2003) and has been utilized for process fault identification in Zhou *et al.* (2004).

In this case study, however, this model is assumed to be *unknown*. Instead, we use this model to generate different faulty working cases to simulate the machining operation. The proposed variation-source identification procedure is applied to these simulated cases to illustrate its effectiveness.

3.2. *Application of the variation-source identification technique*

To demonstrate the proposed variation-source identification technique, the following cases are considered. In each case, the sample size $N = 250$, the dimension of the quality measurement $m = 31$, and $\sigma_\varepsilon = 0.01$. Cases 1 to 6 will be demonstrated to identify those variation sources with a type-A fault signature, cases 7 and 8 will be demonstrated with the use of type-B and type-C fault signatures, respectively. The type-I error for all of the testing in the case study is set at 0.05.

In Table 2, $\sigma_1, \sigma_2, \ldots,$ and σ_6 are the standard deviations of $\mathbf{f}(1), \mathbf{f}(2), \ldots,$ and $\mathbf{f}(6)$, respectively. Based on these parameters, the sample with a sample size of 250 with

Table 2. The considered cases (cases 1 to 8)

	Case							
	1	*2*	*3*	*4*	*5*	*6*	*7*	*8*
σ_1	0.09	0.08	0.005	0.005	0.005	0.005	0.005	0.005
σ_2	0.005	0.08	0.09	0.09	0.005	0.09	0.1	0.005
σ_3	0.005	0.005	0.07	0.005	0.08	0.005	0.005	0.005
σ_4	0.005	0.005	0.08	0.005	0.005	0.06	0.09	0.09
σ_5	0.005	0.005	0.005	0.005	0.005	0.09	0.005	0.08
σ_6	0.005	0.005	0.005	0.005	0.005	0.005	0.005	0.005

workpiece quality measurements $\mathbf{y}$ are generated for each case and the sample covariance matrices are obtained as $\mathbf{S}_1, \mathbf{S}_2, \ldots$ and $\mathbf{S}_8$. We denote the corresponding population covariance matries as $\mathbf{\Sigma}_1, \mathbf{\Sigma}_2 \ldots \mathbf{\Sigma}_8$. Applying the proposed identification method leads to the following results. First we use the MDL criterion to estimate the number of faults for each fault covariance matrix. The results are listed in Table 3.

Table 3 lists MDL(l), $l = 1, \ldots, 5$, for cases 1 to 8. The l that minimizes MDL for each case is the estimated result of the number of significant variation sources. The result is listed in the last row. It can be seen that the number of significant variation sources are correctly identified for each case. The sample covariance matrices for all of the eight cases contain a certain number of faults, so all of them are fault covariance matrices. Based on the number of faults identified using the MDL criterion, we can use the developed variation-source identification procedures to identify the variation sources.

Theorem 1 is intensively used in the variance-source identification procedure. The various testing results are summarized in Table 4.

In case 1, we have $k_1 = 1$ fault. Since there is no fault covariance in the fault library, we simply mark the fault that is detected in $\mathbf{S}_1$ as fault $\{1\}$. The direction of the fault is the eigenvector corresponding to its largest eigenvalue. We put $\mathbf{S}_1$ and its corresponding fault set $\{1\}$ into the fault library.

In case 2, we have $k_2 = 2$ faults. The value of $\dim(\mathcal{F}(\mathbf{\Sigma}_1) + \mathcal{F}(\mathbf{\Sigma}_2))$ is estimated to be two at a level of 0.05. Since $\dim(\mathcal{F}(\mathbf{\Sigma}_1)) = 1$ and $\dim(\mathcal{F}(\mathbf{\Sigma}_2)) = 2$, we have $\dim(\mathcal{F}(\mathbf{\Sigma}_1) \cap \mathcal{F}(\mathbf{\Sigma}_2)) = \dim(\mathcal{F}(\mathbf{\Sigma}_1)) + \dim(\mathcal{F}(\mathbf{\Sigma}_2)) - \dim(\mathcal{F}(\mathbf{\Sigma}_1) + \mathcal{F}(\mathbf{\Sigma}_2)) = 1$. Obviously, $\mathbf{S}_1$ and $\mathbf{S}_2$ share one common fault. There is only one fault (fault $\{1\}$) in $\mathbf{S}_1$, so fault $\{1\}$ should also be contained in $\mathbf{S}_2$ as well. And we further claim a new fault is detected in $\mathbf{S}_2$ and mark this new fault as fault $\{2\}$. $\mathbf{S}_2$ is stored in the fault library for later use and we denote its corresponding fault set as $\{1, 2\}$.

In case 3, we have $k_3 = 3$ faults. We have only two fault covariance matrices in the fault library. The value of $\dim(\mathcal{F}(\mathbf{\Sigma}_1) + \mathcal{F}(\mathbf{\Sigma}_3))$ is estimated as being four. Thus, $\dim(\mathcal{F}(\mathbf{\Sigma}_1) \cap \mathcal{F}(\mathbf{\Sigma}_3)) = \dim(\mathcal{F}(\mathbf{\Sigma}_1)) + \dim(\mathcal{F}(\mathbf{\Sigma}_3)) - \dim(\mathcal{F}(\mathbf{\Sigma}_1) + \mathcal{F}(\mathbf{\Sigma}_3)) = 1 + 3 - 4 = 0$. There is no common fault shared between $\mathbf{S}_1$ and $\mathbf{S}_3$. In another words, fault $\{1\}$ is not contained in $\mathbf{S}_3$. Furthermore, $\dim(\mathcal{F}(\mathbf{\Sigma}_2) + \mathcal{F}(\mathbf{\Sigma}_3))$ is estimated as being four. Hence, we have $\dim(\mathcal{F}(\mathbf{\Sigma}_2) + \mathcal{F}(\mathbf{\Sigma}_3)) = 4$ and then $\dim(\mathcal{F}(\mathbf{\Sigma}_2) \cap \mathcal{F}(\mathbf{\Sigma}_3)) = 2 + 3 - 4 = 1$. Therefore, $\mathbf{S}_2$ and $\mathbf{S}_3$ share one common fault. Because $\mathcal{F}(\mathbf{\Sigma}_1) \cap \mathcal{F}(\mathbf{\Sigma}_3) = \phi$, the common fault shared between $\mathbf{S}_2$ and $\mathbf{S}_3$ should be in a subset of $\mathcal{F}(\mathbf{\Sigma}_2) \sim \mathcal{F}(\mathbf{\Sigma}_1)$. Because only fault $\{2\}$ is contained in $\mathcal{F}(\mathbf{\Sigma}_2) \sim \mathcal{F}(\mathbf{\Sigma}_1)$, the common fault shared between $\mathbf{S}_2$ and $\mathbf{S}_3$ should be fault $\{2\}$. Finally, we identified that fault $\{2\}$ is contained in $\mathbf{S}_3$. In addition, the total number of unidentified faults in $\mathbf{S}_3$ is equal to $\dim(\mathcal{F}(\mathbf{\Sigma}_3)) - 1 = 3 - 1 = 2$ and we claim the other two faults in $\mathbf{S}_3$ are new faults. We mark these two new faults as fault $\{3\}$ and fault $\{4\}$, respectively. Finally, the fault covariance matrix $\mathbf{S}_3$ is put into the fault library together with its fault set identified as $\{2, 3, 4\}$.

In case 4, we have only $k_4 = 1$ fault in $\mathbf{S}_4$. First, the value of $\dim(\mathcal{F}(\mathbf{\Sigma}_1) + \mathcal{F}(\mathbf{\Sigma}_4))$ is estimated as being two. Then $\dim(\mathcal{F}(\mathbf{\Sigma}_2) + \mathcal{F}(\mathbf{\Sigma}_4))$ is estimated as being two and thus $\dim(\mathcal{F}(\mathbf{\Sigma}_2) \cap \mathcal{F}(\mathbf{\Sigma}_4)) = 1$, which shows that there is one common fault shared between $\mathbf{S}_2$ and $\mathbf{S}_4$. Furthermore, the common fault should be a subset of $\mathcal{F}(\mathbf{\Sigma}_2) \sim \mathcal{F}(\mathbf{\Sigma}_1)$. Using similar logic to case 3, we conclude fault $\{2\}$ is contained in $\mathbf{S}_4$. Since $\dim(\mathcal{F}(\mathbf{\Sigma}_4)) = 1$, we stop and store $\mathbf{S}_4$ and its corresponding fault set $\{2\}$ into the fault library.

In case 5, we still have only $k_5 = 1$ fault in $\mathbf{S}_5$. First, the value of $\dim(\mathcal{F}(\mathbf{\Sigma}_1) + \mathcal{F}(\mathbf{\Sigma}_5))$ is estimated as being two and thus $\dim(\mathcal{F}(\mathbf{\Sigma}_1) \cap \mathcal{F}(\mathbf{\Sigma}_5)) = 0$, which means

Table 3. The MDL testing results for cases 1–8

	Case							
	1	*2*	*3*	*4*	*5*	*6*	*7*	*8*
MDL(1)	730.760	6189.368	10 224.591	718.453	650.376	9510.703	9276.650	5258.892
MDL(2)	830.470	807.621	6980.052	827.305	760.555	3871.150	759.455	757.061
MDL(3)	928.074	918.743	896.430	938.041	878.681	974.963	858.304	866.459
MDL(4)	1037.350	1030.352	997.982	1045.741	995.865	1076.330	975.581	978.034
MDL(5)	1143.464	1137.613	1091.076	1155.049	1107.230	1181.825	1086.291	1087.080
Number of faults	1	2	3	1	1	3	2	2

Table 4. The hypothesis testing results of the dimension of the sum of fault spaces

Case	*Null hypothesis*	*s*	T_s	v_s	*Critical value* $\chi^2_{0.95,v_s}$	*Estimated dimension*
2	H_0: $\dim(\mathcal{F}(\Sigma_1)+\mathcal{F}(\Sigma_2)) = s(2 \le s < 3)$	2	33.5960	29	42.5570	2
3	H_0: $\dim(\mathcal{F}(\Sigma_1)+\mathcal{F}(\Sigma_3)) = s(3 \le s < 4)$	3	15 115	28	41.3371	4
	H_0: $\dim(\mathcal{F}(\Sigma_2)+\mathcal{F}(\Sigma_3)) = s$	3	16 619	56	74.4683	4
	$(3 \le s \le 5)$	4	17.2230	27	40.1133	4
4	H_0: $\dim(\mathcal{F}(\Sigma_1)+\mathcal{F}(\Sigma_4)) = s(1 \le s < 2)$	1	20 562	30	43.7730	2
	H_0: $\dim(\mathcal{F}(\Sigma_2)+\mathcal{F}(\Sigma_4)) = s(2 \le s < 3)$	2	30.2360	29	42.5570	2
5	H_0: $\dim(\mathcal{F}(\Sigma_1)+\mathcal{F}(\Sigma_5)) = s(1 \le s < 2)$	1	18 850	30	43.7730	2
	H_0: $\dim(\mathcal{F}(\Sigma_2)+\mathcal{F}(\Sigma_5)) = \mathrm{s}\ (2 \le s < 3)$	2	18 793	29	42.5570	3
	H_0: $\dim(\mathcal{F}(\Sigma_3)+\mathcal{F}(\Sigma_5)) = s(3 \le s < 4)$	3	24.7853	28	41.3371	3
6	H_0: $\dim(\mathcal{F}(\Sigma_1)+\mathcal{F}(\Sigma_6)) = s(3 \le s < 4)$	3	19 540	28	41.3371	4
	H_0: $\dim(\mathcal{F}(\Sigma_2)+\mathcal{F}(\Sigma_6)) = s(3 \le s < 5)$	3	25 314	56	74.4683	4
		4	29.6509	27	40.1133	4
	H_0: $\dim(\mathcal{F}(\Sigma_3)+\mathcal{F}(\Sigma_6)) = s(3 \le s < 6)$	3	17 529	84	106.3948	4
		4	62.4987	54	72.1532	4
	H_0: $\dim(\mathcal{F}(\Sigma_5)+\mathcal{F}(\Sigma_6)) = s(3 \le s < 4)$	3	22 230	28	41.3371	4
7	H_0: $\dim(\mathcal{F}(\Sigma_3)+\mathcal{F}(\Sigma_7)) = s(3 \le s < 5)$	3	59.9664	56	74.4683	3
	H_0: $\dim(\mathcal{F}(\Sigma_6)+\mathcal{F}(\Sigma_7)) = s(3 \le s < 5)$	3	70.2294	56	74.4683	3
	H_0: $\dim(\mathcal{F}(\Sigma_3)+\mathcal{F}(\Sigma_6)+\mathcal{F}(\Sigma_7)) = s\ (3 \le s < 8)$	3	18 422	140	168.6130	4
		4	126.3779	108	133.2569	4
8	H_0: $\dim(\mathcal{F}(\Sigma_4)+\mathcal{F}(\Sigma_8)) = s(2 \le s < 3)$	2	34 543	29	42.5570	3
	H_0: $\dim(\mathcal{F}(\Sigma_4)+\mathcal{F}(\Sigma_6)+\mathcal{F}(\Sigma_8)) = s\ (3 \le s < 6)$	3	101.4221	84	106.3948	3

that no common fault is shared between $\mathbf{S}_1$ and $\mathbf{S}_5$. Second, $\dim(\mathcal{F}(\Sigma_2)+\mathcal{F}(\Sigma_5))$ is estimated as being three and thus $\dim(\mathcal{F}(\Sigma_2)\cap\mathcal{F}(\Sigma_5)) = 0$, which means that no common fault is shared between $\mathbf{S}_2$ and $\mathbf{S}_5$. Furthermore, $\dim(\mathcal{F}(\Sigma_3)+\mathcal{F}(\Sigma_5))$ is estimated as being three and $\dim(\mathcal{F}(\Sigma_3)\cap\mathcal{F}(\Sigma_5)) = 1$, which means there is one common fault shared between $\mathbf{S}_2$ and $\mathbf{S}_5$. Since $\mathbf{S}_4$ contains only $\{2\}$ and we already know that $\{2\}$ is not contained in $\mathbf{S}_5$, we do not have to check $\dim(\mathcal{F}(\Sigma_4)+\mathcal{F}(\Sigma_5))$. Because we know faults $\{3, 4\}$ are contained in $\mathcal{F}(\Sigma_3) \sim \mathcal{F}(\Sigma_1)$ and $\mathcal{F}(\Sigma_3)+\mathcal{F}(\Sigma_4)$, we can only conclude that the common fault between $\mathbf{S}_3$ and $\mathbf{S}_5$ could be either $\{3\}$ or $\{4\}$. But we still cannot conclude that the fault contained in $\mathbf{S}_5$ is $\{3\}$ or $\{4\}$. At this stage fault $\{3\}$ and fault $\{4\}$ cannot be differentiated between.

In case 6, we have $k_6 = 3$ faults. First, $\dim(\mathcal{F}(\Sigma_1)+\mathcal{F}(\Sigma_6))$ is estimated as being four and thus $\dim(\mathcal{F}(\Sigma_1)\cap\mathcal{F}(\Sigma_6)) = 0$, which means that no common fault is shared between $\mathbf{S}_1$ and $\mathbf{S}_6$. Second, because $\dim(\mathcal{F}(\Sigma_2)+\mathcal{F}(\Sigma_6))$ is estimated as being four and thus $\dim(\mathcal{F}(\Sigma_2)\cap\mathcal{F}(\Sigma_6)) = 1$, there is one common fault shared between $\mathbf{S}_2$ and $\mathbf{S}_6$. By the same logic used in case 3, we know that $\{2\}$ is contained in $\mathbf{S}_6$. Furthermore $\dim(\mathcal{F}(\Sigma_3)+\mathcal{F}(\Sigma_6))$ is estimated as being four and thus $\dim(\mathcal{F}(\Sigma_3)\cap\mathcal{F}(\Sigma_6)) = 2$, which means there are two common faults shared between $\mathbf{S}_3$ and $\mathbf{S}_6$. Since $\mathbf{S}_4$ contains only $\{2\}$ and we already know that $\{2\}$ is contained in $\mathbf{S}_6$, we do not have to check $\dim(\mathcal{F}(\Sigma_4)+\mathcal{F}(\Sigma_6))$. Finally, we check $\dim(\mathcal{F}(\Sigma_5)+\mathcal{F}(\Sigma_6))$ and get a value of four and thus $\dim(\mathcal{F}(\Sigma_5)\cap\mathcal{F}(\Sigma_6)) = 0$. There is no common fault shared between $\mathbf{S}_5$ and $\mathbf{S}_6$. If we mark the common fault shared between $\mathbf{S}_3$ and $\mathbf{S}_5$ as $\{3\}$, then $\{3\}$ is not contained in $\mathbf{S}_6$. Now we have $\mathcal{F}(\Sigma_3) \sim \mathcal{F}(\Sigma_5) = \{2, 4\}$, and we conclude that $\{2\}$ and $\{4\}$ are contained in $\mathbf{S}_6$. Because we have already exhausted all of the existing fault labels in the existing fault covariance matrices and find only two historical faults (fault $\{2\}$ and fault $\{4\}$) in $\mathbf{S}_6$. We claim a new fault occurred and mark it as $\{5\}$. Hence, the fault set of $\mathbf{S}_6$ is $\{2, 4, 5\}$. It is important to note that although fault $\{3\}$ and fault $\{4\}$ cannot be differentiated in the previous cases, they are clearly identified from now on. This example shows that not only can historical fault information help us in fault identification; but also that future fault information might also contribute to the identification of historical faults.

Cases 7 and 8 are used to illustrate the applications of type-B and type-C fault signatures.

In case 7, we have $k_7 = 2$ faults. We use a type-B fault signature. Assume that we use a type-B signature of <$\mathbf{S}_3$, $\mathbf{S}_6$, $\mathbf{B}$>. First we test $\dim(\mathcal{F}(\Sigma_3)+\mathcal{F}(\Sigma_7))$ and get a value of three and thus $\dim(\mathcal{F}(\Sigma_3)\cap\mathcal{F}(\Sigma_7)) = 2$. Second, we test $\dim(\mathcal{F}(\Sigma_6)+\mathcal{F}(\Sigma_7))$ and get a value of three and thus $\dim(\mathcal{F}(\Sigma_6)\cap\mathcal{F}(\Sigma_7)) = 2$. Third, we test $\dim(\mathcal{F}(\Sigma_3)+\mathcal{F}(\Sigma_6)+\mathcal{F}(\Sigma_7))$ and get a value of four. Last, we check $\dim(\mathcal{F}(\Sigma_3)+\mathcal{F}(\Sigma_6))$ and get a value of four and faults 2 and 4 are contained in $\mathcal{F}(\Sigma_3)\cap\mathcal{F}(\Sigma_6)$. From Proposition 2, we can check $k_0 = \dim(\mathcal{F}(\Sigma_7)) - \dim(\mathcal{F}(\Sigma_3)+\mathcal{F}(\Sigma_6)+\mathcal{F}(\Sigma_7)) + \dim(\mathcal{F}(\Sigma_3)+\mathcal{F}(\Sigma_6)) = 2$, and thus $k_0 + \mathcal{F}(\Sigma_3)\cap\mathcal{F}(\Sigma_6) = 4$ and equal to $\dim(\mathcal{F}(\Sigma_3)\cap\mathcal{F}(\Sigma_7)) + \dim(\mathcal{F}(\Sigma_3)\cap\mathcal{F}(\Sigma_6))$. Hence, we conclude faults {2} and {4} are contained in $\mathbf{S}_7$. Since $k_7 = 2$, the fault set of $\mathbf{S}_7$ is {2,4}.

In case 8, we have $k_8 = 2$ faults. We will use a type-C fault signature. Assume we use $<\mathbf{S}_6,\mathbf{S}_4,\mathbf{C}>$ as the type-C signature. First we test $\dim(\mathcal{F}(\Sigma_4)+\mathcal{F}(\Sigma_8))$ and get a value of three and thus $\dim(\mathcal{F}(\Sigma_4)\cap\mathcal{F}(\Sigma_8)) = 0$. Second, we test $\dim(\mathcal{F}(\Sigma_4)+\mathcal{F}(\Sigma_6)+\mathcal{F}(\Sigma_8))$ and get a value of three. From Proposition 3, the fault set that corresponds to $\mathcal{F}(\Sigma_6)\sim\mathcal{F}(\Sigma_4)$ is equal to {4, 5}. Because $\dim(\mathcal{F}(\Sigma_8)) - \dim(\mathcal{F}(\Sigma_4)+\mathcal{F}(\Sigma_6)+\mathcal{F}(\Sigma_8)) + \dim(\mathcal{F}(\Sigma_4)+\mathcal{F}(\Sigma_6)) = 2$ and is also equal to $\dim(\mathcal{F}(\Sigma_4)\cap\mathcal{F}(\Sigma_8)) + \dim(\mathcal{F}(\Sigma_6)\sim\mathcal{F}(\Sigma_4))$, we conclude faults {4,5} are contained in $\mathbf{S}_8$.

From the above case studies, we can see that the variation-source identification method developed in this paper is effective and easy to use. The testing procedure for cases 7 and 8 seems more complicated than the testing procedure for cases 1 to 6. However, the use of type-B and type-C fault signatures in those two cases may provide a better utilization of the historical data.

4. Concluding remarks and directions of future study

This paper presented a variation-source identification methodology. The major characteristic of this method is that it does not require a predefined model that links the system measurements and the variation sources. Instead, the method utilizes quality measurement data through the analysis of the eigenspace of the covariance matrices to identify the variation sources. The key steps of the method are the testing of a common part of the eigenspace among multiple covariance matrices and a systematic way to construct fault signatures by applying the testing procedures. A numerical case study is conducted to illustrate the effectiveness of this method. This method can be used in quick root-cause identification of a manufacturing process, which will lead to product quality improvement, production downtime reduction, and hence cost reductions in manufacturing systems.

This paper opens a new direction in variation-source identification technologies. There are still several very interesting open issues related with this method. The first issue is the assumption on the system noise term ε. In this paper, we assume its variance is of the form of $\sigma^2\mathbf{I}$. Although many practical systems can satisfy this requirement (e.g., a system that is very close to linear and the same measurement device being used to measure all the system outputs), some systems (particularly systems with severe nonlinearities) do not have this property. In that case, we have to assume a general form for the covariance matrix of ε. How this general form of the covariance matrix structure will impact on the performance of the testing procedure is not clear. This problem is currently under investigation. The second issue is the impact of sample size. In the case study we have a relatively large sample size ($N = 250$). The testing procedure of Schott (1999) requires a large sample size to have good performance. Bartlett corrections (Jensen, 1993; Cribari-Neto and Cordeiro, 1996; Schott, 1999) have been recommended for smaller sample sizes. More recently, Schott (2003) proposed an alternative testing statistic which is claimed to have a better performance than that of Schott (1999) for small sample sizes. The performance of the developed method could be improved if the new testing method is adopted. The third issue is the continuous improvement of the fault signature. As the number of fault covariance matrices grows, the same fault or fault sets could have multiple signatures. How to combine those multiple signatures together to improve the testing power of the common eigenspace is a very interesting problem. The results on this issue will be reported in the near future.

Acknowledgements

The authors would like to thank the Editors and reviewers for their insightful comments and suggestions, which have significantly improved the paper quality and readability. The authors also gratefully acknowledge the financial support provided by NSF Award DMI-0322147.

References

Apley, D.W. and Lee, H.Y. (2003) Identifying spatial variation patterns in multivariate manufacturing processes: a blind separation approach. *Technometrics*, **45**(3), 220–234.

Apley, D.W. and Shi, J. (2001) A factor-analysis method for diagnosing variability in multivariate manufacturing processes. *Technometrics*, **43**, 84–95.

Boik, R.J. (2002) Spectral models for covariance matrices. *Biometrika*, **89**, 159–182.

Camelio, A.J., Hu, S.J. and Ceglarek, D.J. (2003) Modeling variation propagation of multi-station assembly systems with compliant parts. *ASME Transactions, Journal of Mechanical Design*, **125**, 673–681.

Ceglarek, D. and Shi, J. (1995) Dimensional variation reduction for automotive body assembly. *Journal of Manufacturing Review*, **8**, 139–154.

Ceglarek, D. and Shi, J. (1996) Fixture failure diagnosis for autobody assembly using pattern recognition. *Transactions of the ASME, Journal of Engineering for Industry*, **188**, 55–65.

Chiang, L.H., Russell, E.L. and Braatz, R.D. (2001) *Fault Detection and Diagnosis in Industrial Systems*, Springer, London, UK.

Cribari-Neto, F. and Cordeiro, G.M. (1996) On Bartlett and Bartlett-type corrections, *Econometric Reviews*, **15**, 339–367.

Ding, Y., Ceglarek, D. and Shi, J. (2000) Modeling and diagnosis of multistage manufacturing processes: part I state space model. *Presented at the 2000 Japan/USA Symposium on Flexible Automation*, July 23–26, Ann Arbor, MI, paper 2000JUSFA-13146.

Ding, Y., Ceglarek, D. and Shi, J. (2002) Fault diagnosis of multistage manufacturing processes by using state space approach. *Transactions of the ASME, Journal of Manufacturing Science and Engineering*, **124**, 313–322.

Djurdjanovic, D. and Ni, J. (2001) Linear state space modeling of dimensional machining errors. *Transactions of NAMRI/SME*, **29**, 541–548.

Flury, B.N. (1987) Two generalizations of the common principal component model. *Biometrika*, **74**(1), 59–69.

Huang, Q., Zhou, N. and Shi, J. (2000) Stream of variation modeling and diagnosis of multi-station machining processes, in *Proceedings of IMECE 2000*, MED Vol. 11, Orlando, FL, pp. 81–88.
Jensen, J.L. (1993) A historical sketch and some new results on the improved likelihood statistic. *Scandinavian Journal of Statistics*, **20**, 1–15.
Jin, J. and Shi, J. (1999) State space modeling of sheet metal assembly for dimensional control. *Transactions of the ASME*, *Journal of Manufacturing Science and Engineering*, **121**, 756–762.
Jin, N. and Zhou, S. (2005) Data-Driven variation source identification of Manufacturing Processes Based on Eigenspace Comparison, submitted *Naval Research Logistics*, in revision.
Krzanowski, W.J. (1979) Between-groups comparison of principal components. *Journal of the American Statistical Association*, **74**, 703–707.
Krzanowski, W.J. (1982) Between-groups comparison of principal components—some sampling results. *Journal of Statistical Computation and Simulation*, **15**, 141–154.
Mantripragada, R. and Whitney, D.E. (1999) Modeling and controlling variation propagation in mechanical assemblies using state transition models. *IEEE Transactions on Robotics and Automation*, **15**, 124–140.
Montgomery, D.C. and Woodall, W.H. (eds.) (1997) A discussion on statistically-based process monitoring and control. *Journal of Quality Technology*, **29**, 121–162.
Raich, A.C. and Cinar, A. (1995) Multivariate statistical methods for monitoring continuous processes: assessment of discrimination power of disturbance models and diagnosis of multiple disturbances. *Chemometrics and Intelligent Laboratory Systems*, **30**(1), 37–48.
Rong, Q., Ceglarek, D. and Shi, J. (2000) Dimensional fault diagnosis for compliant beam structure assemblies. *Transactions of the ASME Journal of Manufacturing Science and Engineering*, **122**, 773–780.
Russell, E.L. and Braatz, R.D. (1998) Fault isolation in industrial processes using Fisher discriminant analysis, in *Foundations of Computer-Aided Process Operations*. Pekny J.F. and Blau, G.E. (eds), American Institute of Chemical Engineers. New York, NY, pp. 380–385.
Schott, J.R. (1988) Common principal component subspaces in two groups. *Biometrika*, **75**(2), 229–236.
Schott, J.R. (1991) Some tests for common principal component subspaces in several groups. *Biometrika*, **78**(3), 771–777.
Schott, J.R. (1997) *Matrix Analysis for Statistics*, Wiley, New York, NY.
Schott, J.R. (1999) Partial common principal component subspaces. *Biometrika*, **86**(4), 899–908.
Schott, J.R. (2003) Weighted chi-squared tests for partial common principal component subspaces. *Biometrika*, **90**(2), 411–421.
Woodall, W.H. and Montgomery, D.C. (1999) Research issues and ideas in statistical process control. *Journal of Quality Technology*, **31**, 376–386.
Zhou, S., Chen, Y. and Shi, J. (2004) Statistical estimation and testing for variation root cause determination of multistage manufacturing processes. *IEEE Transactions on Automation Science and Engineering*, **1**, 73–83.
Zhou, S., Huang, Q. and Shi, J. (2002) State space modeling of dimensional variation propagation in multistage machining process using differential motion vectors. *IEEE Transactions on Robotics and Automation*, **19**(2), 296–309.

Appendix

Proof of Theorem 1. The main steps of the proof follow those of the proof in Schott (1999). In Schott (1999), the author has proved the following results: given g samples of m variables of normally distributed quality measurements, the sample and population covariance matrices of these g samples are $\mathbf{S}_i$ and $\boldsymbol{\Sigma}_i$ ($i = 1, 2, \ldots, g$), and each sample covariance matrix needs k principal components to explain the major variations in each group. If H_{0s} is true, then T_s has a chi-squared distribution with $v_s = (kg - s)$ $(\mathrm{m} - s)$ degrees of freedom, where T_s is defined in Equation (5). By the definition of the fault vectors and fault space, this result is very similar to Theorem 1 except that it requires that all of the sample covariance matrices have the same number (k) of principal components to explain the major variations. However, this is not a severe limitation of this derivation. After replacing k and gk with k_i and $\sum_{i=1}^{g} k_i$ respectively, similar derivations can be obtained to prove Theorem 1. Another difference is that we used $\max(k_i)$ as the lower boundary of s in Theorem 1. The rationale is that the sum fault space spanned by all of the fault vectors of covariance matrices should have its dimension greater than or equal to the maximal dimension of each individual fault space provided that all of the faults contained in a fault covariance matrix are independent. ∎

Biographies

Nong Jin is a Ph.D. student in the Department of Industrial and Systems Engineering at University of Wisconsin-Madison. His research interests focus on statistical modeling and variation source identification in large complex systems.

Shiyu Zhou is an assistant professor in the Department of Industrial and Systems Engineering at the University of Wisconsin-Madison. He got his B.S. and M.S. in Mechanical Engineering at University of Science and Technology of China in 1993 and 1996 respectively, and got his Master in Industrial Engineering and Ph.D. in Mechanical Engineering at the University of Michigan in 2000. Dr. Zhou's research interests are the in-process quality and productivity improvement methodologies by integrating statistics, system and control theory, and engineering knowledge. The objective is to achieve automatic process monitoring, diagnosis, compensation, and their implementation in various manufacturing processes. His research is sponsored by National Science Foundation, Department of Energy, NIST-ATP, and industries. Dr. Zhou is a member of IIE, INFORMS, ASME, and SME.

Contributed by the Process Monitoring and Control Department